Carrier transport in thin films of silicon nanoparticles

T. A. Burr, A. A. Seraphin, E. Werwa, and K. D. Kolenbrander

Department of Materials Science and Engineering, Massachusetts Institute of Technology, Cambridge, Massachusetts 02139

(Received 25 April 1997)

The electrical and electroluminescence characteristics of heterostructure systems containing thin films of visibly emitting silicon nanoparticles are shown to be controlled by carrier transport through the nanoparticulate films. A conduction mechanism encompassing both geometric and electronic effects most effectively relates the high resistivity with structural properties of the films. Heterostructure devices are constructed with silicon nanoparticle active layers produced by pulsed laser ablation supersonic expansion. The observed temperature-dependent photoluminescence, electroluminescence, and I-V characteristics of the devices are consistent with a model in which carrier transport is controlled by space-charge-limited currents or tunneling through potential barriers on a percolating lattice. [S0163-1829(97)00132-X]

I. INTRODUCTION

Nanostructured silicon has emerged as a material of great interest in recent years because it exhibits efficient photoluminescence (PL) and thus has potential for use in silicon-based photonic and optoelectronic platforms.[1–7] One of the greatest challenges has been the integration of nanoscale silicon materials into serviceable architectures such as electroluminescent (EL) devices. We have previously reported the construction of light-emitting devices employing self-supporting thin films of silicon nanoparticles (nano-Si) as the active layer between an aluminum–indium tin oxide (ITO) electrode pair.[8] The low light emission efficiency observed from these devices is thought to result from inefficient carrier supply to the active light-emitting region; the contribution of nonradiative recombination of carriers within the nano-Si layer is minimal in comparison. Prospects for rational device design and improvement depend on gaining a greater understanding of the electrode/nano-Si interface, which controls carrier injection efficiency, as well as the bulk electrical and optical properties of the films, which can influence carrier transport and luminescence efficiency.

Studies of porous silicon (PS) based light-emitting devices have provided some insight into the electrical characteristics of nanostructured silicon. The current-voltage (I-V) characteristics and luminescence efficiency of certain devices have been shown to be limited by transport within the PS layer. However, the actual conduction mechanism in nanostructured silicon thin films remains a largely open question, and the significant differences between the PS materials under investigation complicate any general interpretation. For example, Fowler-Nordheim tunneling,[1] Poole-Frenkel,[9] and space-charge limited[10,11] behaviors have been demonstrated for similar device constructions, and the discrepancy between these transport mechanisms has been shown to result from the various formation and processing steps used to mechanically stabilize the low volume-fraction PS films.

The use of a nonequilibrium gas phase source of silicon nanoparticles provides an opportunity to contribute to the understanding of conduction mechanisms in nanostructured silicon films. In contrast to porous silicon, this synthesis and processing path produces high-density, self-supporting thin films of silicon nanoparticles that may be deposited on a wide range of electrode systems. Because laser ablated films do not require a Si substrate, it is possible to investigate directly the role of both electrode/nano-Si interfaces through substitution of electrode materials. Contacts can be tailored to obtain the desired electrical behavior, as they control whether the current is limited by carrier injection into or carrier transport through the film. Carrier transport in PS has been attributed to the electronic properties of the material and/or the geometry of the connecting network. It is not immediately evident that the same mechanistic framework should be applied to the nano-Si films since they are microstructurally quite different. The laser-ablated nanoparticulate Si does not consist of interconnecting wirelike structures, but rather separate particles, which may consequently effect both the topological and energetic aspects of carrier transport.

The temperature-dependent PL, EL, and electrical characteristics of the nanoparticulate Si films will be evaluated herein. The PL data provide strong evidence for carrier confinement, and EL results indicate that device characteristics rather than nonradiative recombination dominate the luminescence intensity. The electrical properties show that carrier transport through the nano-Si films is predominant over electrode/interface effects in controlling device performance. The low conductivity is attributed to a combination of electronic and geometric effects which can be effectively represented by tunneling or space-charge-limited currents on a percolating lattice. This proposed conduction mechanism establishes a relationship between the electronic and microstructural properties of the films. Similarities between the electrical properties of laser-ablated and porous silicon are remarkable considering the microstructural differences between the two nanostructured materials systems.

II. EXPERIMENTAL METHODS

Pulsed laser ablation supersonic expansion was employed to deposit thin nanoparticulate silicon films.[12] In a high vacuum chamber, isolated nanoparticles with unpassivated surfaces were deposited onto substrates placed in the path of the expansion. Substrates were varied according to charac-
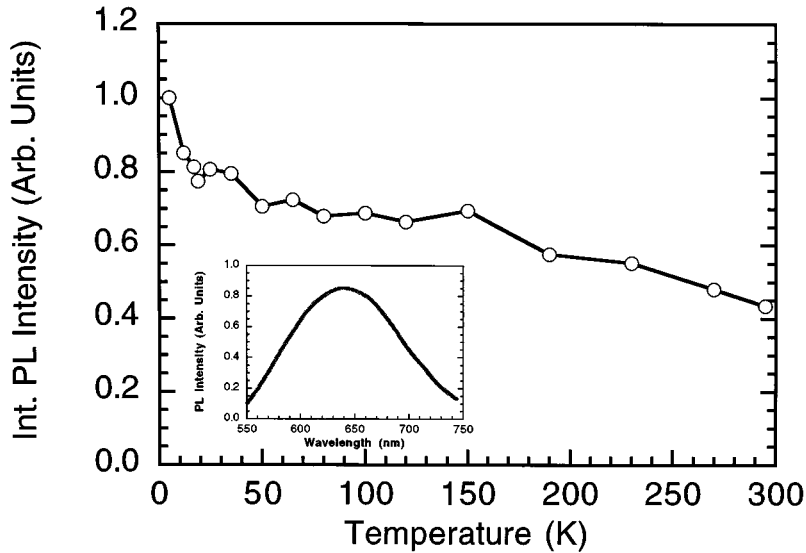
FIG. 1. Integrated photoluminescence emission intensity from a film of silicon nanoparticles as a function of temperature. The emission intensity increases with decreasing temperature, indicating an enhancement of radiative recombination. The very weak temperature dependence is evidence of enhanced exciton confinement. A typical room-temperature photoluminescence spectrum is shown in the inset.

terization or device requirements. For photoluminescence work, films were grown on Teflon, while p-type silicon wafers (10–20 Ω cm), aluminum sheet, or patterned ITO/glass substrates were used for the EL, electrode, and carrier transport studies. An Ohmic contact was formed on the back side of the p-type silicon substrates prior to nano-Si film deposition. The films consisted of size-dispersed nanoclusters which grow a native oxide layer once removed from vacuum.

The PL samples were first treated with 48 wt % HF for ~30 s to remove the initial oxide. The surface of the samples was then reoxidized by immersing them in 20 wt % nitric acid for ~1 min. PL characterization was performed in a cryostat, allowing the temperature of the samples to be varied between 4 and 300 K. A pulsed 3×Nd:YAG (yttrium aluminum garnet) laser ($\lambda_{ex} = 355$ nm) was used as an excitation source, operating at 1.5 mJ/pulse with a 7-nsec pulse width and a spot size of ~1 cm^2. Luminescence spectra, taken using a 0.275-m monochromator coupled with a Si photodiode array detector cooled to −20 °C, were corrected for monochromator and detector response.

Simple three-layer heterostructure devices were employed in the electrode and carrier transport studies. Self-supporting thin films of silicon nanoparticles (100–200 nm thick) were deposited on the appropriate substrate. A ~200-nm-thick aluminum layer was evaporated to form a top electrode with a 4 mm^2 square or 3 mm^2 round active area. Current-voltage characteristics were measured in a two-terminal configuration using standard semiconductor parameter analysis techniques. Room-temperature and temperature-dependent I-V studies were conducted under an inert He atmosphere in the cryostat described for PL. EL light output was measured with a silicon photodiode placed ~1 mm from the device.

III. RESULTS AND DISCUSSION

A. Temperature dependence of PL and EL intensity

The PL behavior of nanoparticulate Si films can reveal a great deal about the recombination mechanisms in the nanostructures. Extensive studies on the role of particle size and surface in the visible PL behavior of nano-Si films implicate

a quantum-confinement-based model as the source of the efficient luminescence exhibited by this material.[13,14] The PL peak blueshifts as particle size is reduced, which is consistent with a quantum-confined system. Oxide or surface-state luminescence mechanisms can be ruled out as nanoparticle surface species control only the intensity of the PL, not the emission wavelength. This to be expected, as the pulsed laser ablation supersonic expansion technique is well suited for the production of particles that fall within the relevant size range for quantum confinement[15] and the existence of these particles has been confirmed in nano-Si films.[12]

The temperature dependence of the PL behavior can provide additional information about the carrier recombination mechanism. As shown in Fig. 1, the integrated PL intensity of a nano-Si film increases with decreasing temperature as a result of the suppression of lattice vibrations at low temperatures, which favors radiative transitions. This very weak temperature dependence of the emission intensity is further evidence of carrier confinement and the resultant enhanced exciton-binding energy predicted for quantum-confined systems.[16] The binding energy has been calculated to be ~200 meV in ~2 nm silicon particles, well above room-temperature thermal energy, so excitons that in the bulk would rapidly thermalize could exist to much higher temperatures in nanoscale systems. Weakly temperature-dependent PL has been observed in other quantum-confined semiconductor systems including CdS quantum dots[17] and $Si_{1-x}Ge_x$ quantum wells.[18] This electronic localization should also influence the transport properties of the films.

In contrast, the EL intensity is found to increase with increasing temperature, as shown in Fig. 2. The temperature dependence of the EL encompasses the temperature dependence of both the PL (i.e., radiative versus nonradiative recombination) and the electrical properties of the Si nanoparticle films. Since EL intensity increases as temperature increases, despite the increased probability of nonradiative recombination, some aspect of carrier motion through the heterostructure must affect the EL intensity. The electrical characteristics of the devices arise both from injection at the electrode/active layer interfaces and from carrier transport through the nano-Si film. It is critical to identify which of
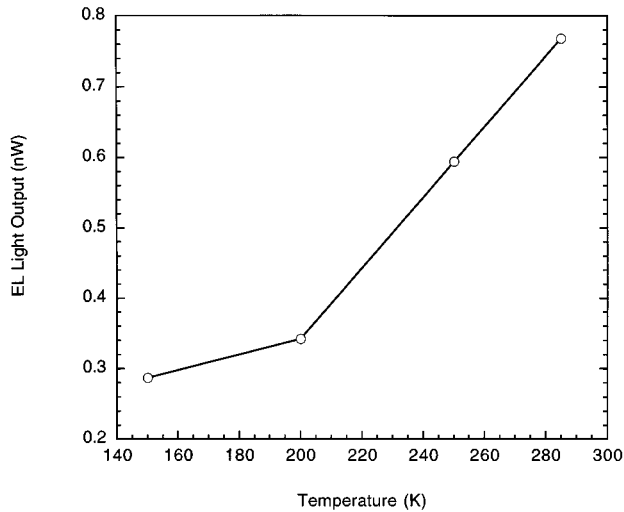
FIG. 2. The temperature dependence of the EL output power for an Al/Si nanoparticle/ITO device driven at 10 V. Light output increases with increasing temperature and is directly proportional to the current.

these mechanisms limits the performance of our devices if improvements are to be made.

B. Electrode effects

The heterostructure devices examined in this study can be thought of as two metal-semiconductor junctions, with the nano-Si layer serving as the common semiconductor layer. The I-V characteristics of such junctions are determined by the alignment of the Fermi levels in the two materials, and classically, they can be either Ohmic or rectifying. Electrode materials are expected to show different behaviors depending on the position of the Fermi level (work function) in each. To ascertain the importance of the nano-Si/electrode heterojunction, devices using different electrode combinations

were constructed. The electrode pairs investigated include Al/p-type Si, Al/Al, and Al/ITO.

The dc I-V curve of a p-type Si/nano-Si film/Al heterostructure, a structure similar to that of many PS-based devices, is shown in Fig. 3(a). The device exhibits rectifying behavior, although the rectifying ratio is low ($I_F/I_R \sim 100$ at 10 V). The I-V characteristics of this device can be represented as a serial combination of a diode and resistor:

$$I = I_0 \exp[q(V - IR)/nkT], \qquad (1)$$

where I_0 is the saturation current in reverse bias, n is the ideality factor, and R is a resistance usually assumed to be independent of applied voltage. A fit based on Eq. (1) is given by the solid line in Fig. 3(a). Although the general behavior of the I-V curve is reproduced, the ideality factor is ~ 33. This high value suggests that most of the applied voltage does not drop on the barrier, but rather on the nanoparticulate silicon layer.

These results are consistent with a model proposed by Ben-Chorin, Möller, and Koch for a comparable metal-porous silicon system,[19] in which the diodelike behavior originates from the Ps/c-Si interface and the Al/PS interface forms a quasi-Ohmic contact. The reverse bias current is limited by the diode, resulting in rectifying characteristics. Under forward bias, the applied voltage is larger than any reasonable barrier; thus the diode term becomes negligible and the majority of voltage drops on the resistor. Current flow through the resistor (the PS film) is strongly field dependent.

To avoid the difficulties presented by the rectifying nano-Si/c-Si junction, the I-V characteristics of an Al/nano-Si film/Al heterostructure were evaluated, as shown in Fig. 3(b). When Al is exchanged for the p-type Si substrate, the I-V curve becomes non-Ohmic and nonrectifying. Assuming that carrier injection at the Si-nanoparticle/Al heterojunction is essentially Ohmic, a device with electrode controlled conduction should exhibit a linear, Ohmic I-V curve. This is not the behavior that is observed, which implies that for the
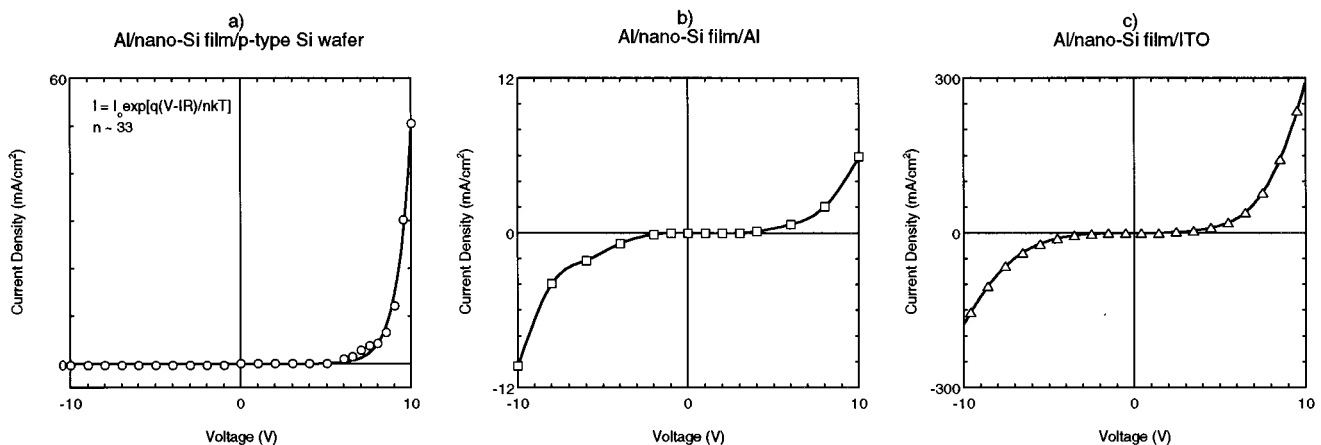
FIG. 3. The room-temperature I-V characteristics of (a) Al/Si nanoparticles/p-type Si, (b) Al/Si nanoparticles/Al, and (c) Al/Si nanoparticles/ITO. For each of the three electrode pairs, the Al electrode was connected to the negative lead and the alternate electrode adjoined the positive lead. Curve (a) exhibits rectifying, interface limited behavior. The solid line is the best fit to Eq. (1), which describes the serial combination of a diode and a resistor. In contrast, transport through the nanoparticle film determines the I-V characteristics of (b) and (c). Traces (b) and (c) are fit with a cubic spline (solid line) to aid the eye.

Al/Al electrode system, current is limited by carrier transport through the nano-Si film in both forward and reverse bias.

The *I-V* trace of the Al/nano-Si film/ITO device [Fig. 3(c)], constructed to permit observation of light output from the device, shows the same kind of non-Ohmic, nonrectifying behavior as the Al/Al electrode system. This is not surprising since the work functions of Al (4.26 eV) and ITO (4.5–4.7 eV) are comparable,[20] and the two materials should thus behave similarly with respect to carrier injection. Further indication that the Al/nano-Si film/ITO device operates in the carrier transport limited regime under forward bias was previously evidenced in the linear relationship between output power and current density, and the long transit times (on the order of tens of μs for films 150–200 nm thick).[21]

The low conductivity of nanostructured silicon is a result of the reduced effective mobility (μ_{eff}) compared to bulk silicon.[10,22] This is favorable for PL, as it is more difficult for carriers to drift apart, bypassing luminescent pathways. However, μ_{eff} places great constraints on EL, since radiative recombination depends, in part, on carriers encountering each other as they move through the film. It is not surprising then, that EL efficiency is directly proportional to the effective mobility. When operating in the transport-limited regime, the time it takes for carriers to traverse the film (τ_t) is described by the equation

$$\tau_t = d^2/\mu_{\text{eff}}V, \qquad (2)$$

where V is the applied bias and d is the film thickness. This relationship assumes a single electron-hole mobility, although the argument is essentially the same if the mobilities are unequal. Transit times on the order of 10 μs have been measured for nano-Si-based devices with an observed power efficiency of $\sim 10^{-4}\%$.[21] According to Eq. (2), this corresponds to a μ_{eff} of 10^{-6} cm^2/V s for the laser-ablated nanoparticulate silicon films. Porous silicon films in similar metal/PS devices report a μ_{eff} on the order of 10^{-4} cm^2/V s with power efficiencies estimated to be on the order of $10^{-2}\%$.[1,10,23] This direct correlation demonstrates that improvements in device performance will require increased carrier motion through the silicon nanostructures.

C. Carrier transport

The electrical characteristics of the Al/nano-Si film/ITO device are limited by carrier transport through the laser-ablated nano-Si film. Understanding the carrier transport mechanism is thus critical both for engineering improved devices and for determining the origin of the high nanoparticulate Si film resistivity. Presumably electronic and/or geometric constraints contribute to the reduced carrier mobility in the films. Nano-Si films consisting of a collection of size-disperse quantum-confined particles may have significant energy-gap variations from one particle to the next, and the methods carriers employ to traverse these interparticle barriers theoretically have distinct temperature dependencies. For example, if hopping is the transport mechanism, the broad distribution of localized electronic states will lead to a large range of trapping and release times. This type of temporal dispersion tends to imply large temperature dependencies, since emission from traps is a strongly temperature-dependent process. At the other extreme, the topological
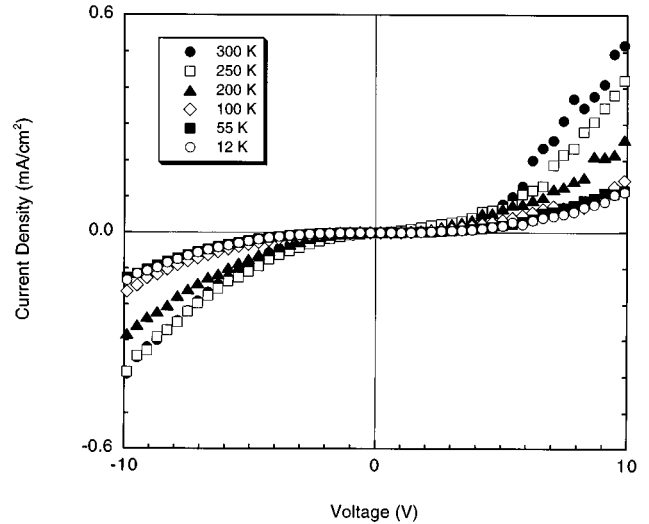
FIG. 4. The temperature-dependent *I-V* characteristics of an Al/Si nanoparticle/ITO electroluminescent device. The *I-V* behavior exhibits a weak temperature dependence which is non-Ohmic and nonrectifying at all temperatures. The device emits yellow-orange light in both forward and reverse biases.

structure imposed by the Si skeleton may limit carrier mobility. A mechanism that is entirely geometric and not electronic in origin has no intrinsic temperature dependence. Thus, temperature dependence is one of the defining experiments to be performed.

The temperature-dependent *I-V* behavior of an Al/nano-Si film/ITO device was studied to help elucidate the governing carrier transport mechanisms. As shown in Fig. 4, the *I-V* characteristic is non-Ohmic and nonrectifying from 4 to 300 K, which indicates that carrier transport dominates the dc electrical characteristics over this temperature range. At temperatures of 100 K and below, the *I-V* characteristics are essentially independent of temperature, while above 100 K, there is a slight increase in current density with increasing temperature for applied bias greater than 5 V. Similar behavior has also been observed in Si-rich SiO$_2$ films[24,25] and certain porous silicon samples.[10] However, this observation is not universal, as nanostructured silicon materials are fabricated with a broad range of structures and surface passivations which may contribute to the variety of observed transport mechanisms. For example, the *I-V* characteristics of other PS films are strongly temperature dependent, with the current-density changing three orders of magnitude over the 200–300 K temperature range.[9]

The weakly temperature-dependent current density observed in this study implies the resistivity is topological in nature and/or that conduction processes which are not thermally activated, such as space-charge limited current or tunneling between Si nanoparticles, are present. On one hand, the PL data strongly suggest that similar to amorphous semiconductors, the nano-Si films consist of a spectrum of localized states that will almost certainly provide some electronic contribution to the carrier transport process. On the other hand, the temperature dependence of the *I-V* behavior of nanoparticulate silicon is small in comparison to other dispersive transport systems such as hydrogenated amorphous Si. This may be evidence for carrier mobility reduction via

a)

b)
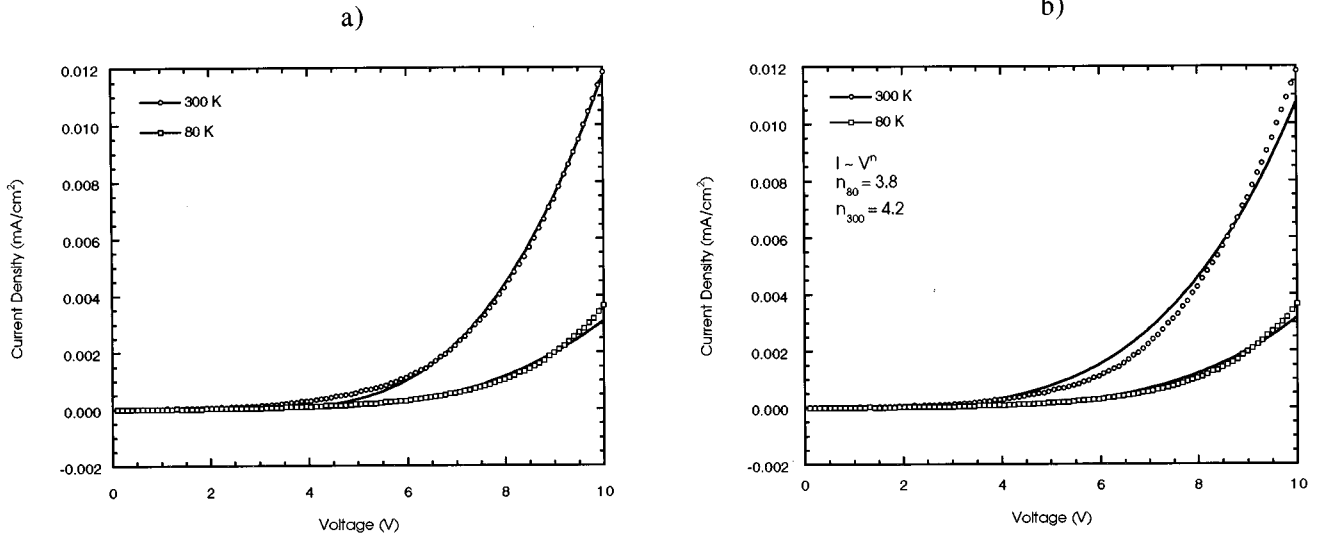
FIG. 5. The dc I-V traces of an Al/Si nanoparticle/ITO heterostructure at 300 and 80 K. Experimental values are marked by the unfilled points. The solid lines represent the best curve fit at the given temperature to (a) the FN tunneling relation $I \sim V^2 \exp(-b/V)$; and (b) the SCLC equation $I \sim V^n$, with the resultant fitting parameter, $n \sim 4$.

purely spatial disorder, as opposed to a combination of geometric and electronic elements. A similar temperature dependence has been observed in certain PS samples, and the researchers cite purely topological constraints as a satisfactory starting point for explaining their measurements.[26] In another set of PS devices exhibiting strongly temperature-dependent I-V characteristics, the electrical behavior was attributed to a combination of electronic and geometric effects, with each dominating in different regimes.[22] It is thus necessary to consider both mechanisms when describing carrier transport in the laser-ablated nano-Si films.

1. Topological effects

When describing possible conduction processes in nanoparticulate solids, it is vital to account for the microstructure of the material. It is well known that conductivity in spatially disordered materials can be modeled by percolation effects. In very general terms, a sample is regarded as being made up of clusters, where a cluster is any set of connected vertices. The key phenomenon in percolation theory is the existence of a threshold: at a critical concentration an infinite cluster (a connected path that extends throughout the sample) forms. In the nanoparticulate Si films, the vertices are an aggregate of randomly distributed and contacting particles through which charge carriers attempt to pass when an electric field is applied. Because the films are built up particle by particle, it is reasonable to assume that they operate above the percolation threshold and that some conductivity pathways through the film exist. In accordance with the theory of percolation conductivity, the films are modeled as by a network of resistors. Carriers will follow the path of least resistance through the film and current will be carried in regions of relatively high local conductivity which occur only in a small fraction of the material, resulting in a diminished drift velocity. A variety of models may be invoked to describe percolation-based behavior,[27] and although a quantitative analysis would require extensive ac conductivity measurements, qualitatively,

all dictate that the spatial constraints imposed by the Si skeleton will be manifested in terms of a reduced dc conductivity.[22]

2. Electronic effects

For electrical conduction to occur, carriers have to be transferred from one particle to the next across an energetic barrier. The observed weak temperature dependence in the I-V characteristics of the nano-Si films implicates tunneling through these barriers or space-charge transfer as probable mechanisms, since other models would depend exponentially on temperature.

Fowler-Nordheim (FN) tunneling is caused by field ionization of trapped electrons into a conduction band. Current due to tunnel emission should have essentially no temperature dependence, but should be dependent on the expression[28]

$$I \sim V^2 \exp(-b/V). \qquad (3)$$

Figure 5(a) shows that reasonable agreement is obtained between the experimental data and Eq. (3). The b value encompasses an effective mass term and a barrier height. Assuming $m^* = m_0$, even the best fits to the data yielded barrier heights on the order of 37 eV, which is physically unreasonable. Most realistic barrier heights can only be obtained for physically inappropriate values of $m^* \sim 0.0001 m_0$. However, the FN model is a classical description; it does not account for geometric and charging effects nor is it equipped to deal with the fact that confinement of carriers in nanoparticulate silicon may prevent the formation of traditional conduction band. Thus, tunneling between nanoparticles can still be considered a valid potential transport mechanism. In addition, tunneling is generally more sensitive to separation distance than thermal emission mechanisms, and tunneling current will exceed the thermally generated current if the separation distance between particles is small enough (i.e., on the order

of angstroms).[29] This condition is satisfied as the particles in the nano-Si film are in contact, which also supports a tunneling current dominated model.

Space-charge-limited currents (SCLC) can occur in highly insulating substances when carriers are injected and no compensating charge is present. They are generally described by[30]

$$I = aV + bV^n. \qquad (4)$$

The first term in Eq. (4) dominates at low fields, resulting in Ohmic behavior, while at high fields the second term controls the I-V characteristics and the equation simplifies to $I \sim V^n$ ($n > 1$). The parameter n is related to the distribution of localized states in the insulator: a narrowing of the distribution is manifested in an increase in n. Large values of n are indicative of a slowly varying energetic distribution, resulting in a more uniform distribution of the space-charge density between cathode and anode.[31]

Carrier transport in PS-based devices exhibiting weakly temperature-dependent I-V behavior, similar to that of the nano-Si films,[10] has been attributed to SCLC, with values of n ranging from 2 to 3.[10,11,32] When I-V curves from the laser-ablated films are evaluated using the space-charge model [Fig. 5(b)], quantities of $n \sim 4$ are obtained. Data from polycrystalline diamond films with grain sizes on the order of micrometers have also been fit to this equation with $n = 4.2$.[33] The larger n value exhibited by the nano-Si films indicates that carriers move through a more uniform energetic (size) distribution than that of PS; however, it may be the larger particles providing the path of least resistance. If the majority of current in the nano-Si films is being carried in bigger particles, bypassing smaller ones and thus shunting out the luminescent pathways, this would be consistent with the observed low EL efficiency.

IV. CONCLUSIONS

The temperature-dependent I-V behavior of the nano-Si films may be adequately described in terms of conductivity on a spatially constraining percolation-type lattice. Carrier transport occurs via SCLC or tunneling and the constraining nano-Si film geometry further reduces the dc conductivity. Both the space-charge and the tunneling-based models qualitatively describe the nano-Si film data; however, these models do not encompass geometric effects and charging effects (which may be large when particles are in the quantum confined range).[34–37] The data presented in this study, coupled with the existing PS literature, suggest that a combination of both geometric and electronic effects must be taken into account when describing conductivity in nanoscale Si films. The similarities between the electrical properties of laser-ablated and porous silicon are significant, and unexpected considering the microstructural differences between the two nanoscale materials systems.

EL and electrode studies indicate that conduction through the laser-ablated nano-Si films dominates over interface effects or nonradiative recombination in controlling device performance. The low EL efficiency implies that carriers prefer to move through large particles, which greatly reduces the probability of carriers meeting in smaller particles to recombine radiatively. The PL data show strong evidence of carrier confinement, which is reflected in the transport properties. Although carrier localization is advantageous for PL, EL device performance is adversely affected by the resistive nature of the nano-Si films. As such, improvements will require a way to enhance conduction between Si nanoparticles, through the development of more sophisticated device architectures or the incorporation of the particles into semiconductor host matrices.[38]

[1] L. Tsybeskov, S. P. Duttagupta, K. D. Hirschman, and P. M. Fauchet, Appl. Phys. Lett. **68**, 2058 (1996).

[2] H. Mimura, T. Matsumoto, T. Futagi, and Y. Kanemitsu, J. Phys. Soc. Jpn. **63**, 203 (1994).

[3] W. Lang, P. Steiner, and F. Kozlowski, J. Lumin. **57**, 341 (1993).

[4] N. Koshida, H. Koyama, Y. Yamamoto, and G. J. Collins, Appl. Phys. Lett. **63**, 2655 (1993).

[5] F. Namavar, H. P. Maruska, and N. M. Kalkhoran, Appl. Phys. Lett. **60**, 2514 (1992).

[6] N. Koshida and H. Koyama, Appl. Phys. Lett. **60**, 347 (1992).

[7] A. Loni, A. J. Simons, T. I. Cox, P. D. J. Calcott, and L. T. Canham, Electron. Lett. **31**, 1288 (1995).

[8] T. A. Burr, A. A. Seraphin, and K. D. Kolenbrander, in *Advanced Luminescent Materials, Electrochemical Society Proceedings*, edited by D. J. Lockwood, P. M. Fauchet, N. Koshida, and S. R. J. Brueck (The Electrochemical Society, Pennington, NJ, 1996), Vol. 95-25, p. 324.

[9] M. Ben-Chorin, F. Möller, and F. Koch, Phys. Rev. B **49**, 2981 (1994).

[10] C. Peng, K. D. Hirschman, and P. M. Fauchet, J. Appl. Phys. **80**, 295 (1996).

[11] L. Tsybeskov, S. P. Duttagupta, and P. M. Fauchet, Solid State Commun. **95**, 429 (1995).

[12] E. Werwa, A. A. Seraphin, L. A. Chiu, C. Zhou, and K. D. Kolenbrander, Appl. Phys. Lett. **64**, 1821 (1994).

[13] A. A. Seraphin, E. Werwa, and K. D. Kolenbrander, J. Mater. Res. (to be published).

[14] A. A. Seraphin, S.-T. Ngiam, and K. D. Kolenbrander, J. Appl. Phys. **80**, 6429 (1996).

[15] M. F. Jarrold and J. E. Bower, J. Chem. Phys. **96**, 9180 (1992).

[16] T. Takagahra and K. Takeda, Phys. Rev. B **46**, 15 578 (1992).

[17] A. Eychmüller, A. Hasselbarth, L. Katskias, and H. Weller, J. Lumin. **48**, 745 (1991).

[18] S. Fukatsu, J. Cryst. Growth **157**, 1 (1995).

[19] M. Ben-Chorin, F. Möller, and F. Koch, J. Appl. Phys. **77**, 4482 (1995).

[20] I. D. Parker, J. Appl. Phys. **75**, 1656 (1994).

[21] T. A. Burr and K. D. Kolenbrander, in *Surface/Interface and Stress Effects in Electronic Material Nanostructures*, edited by S. M. Prokes, R. C. Cammarata, K. L. Wang, and A. Christou, MRS Symposia Proceedings No. 405 (Materials Research Society, Pittsburgh, 1996), p. 271.

[22] M. Ben-Chorin, F. Möller, and F. Koch, Phys. Rev. B **51**, 2199 (1995).

[23] C. Peng and P. M. Fauchet, Appl. Phys. Lett. **67**, 2515 (1995).

[24] D. J. DiMaria, J. R. Kirtley, E. J. Pakulis, D. W. Dong, T. S. Kuan, F. L. Pesavento, T. N. Theis, and J. A. Cutro, J. Appl. Phys. **56**, 401 (1984).

[25] E. W. Forsythe, E. A. Whittaker, D. Morton, B. A. Kahn, B. S. Sywe, Y. Lu, S. Liang, C. Gorla, and G. S. Tompa, in *Surface/Interface and Stress Effects in Electronic Material Nanostructures* (Ref. 21), p. 253.

[26] P. Rao, E. A. Schiff, L. Tsybeskov, and P. M. Fauchet, in *Advances in Microcrystalline and Nanocrystalline Semiconductors, 1996*, edited by P. M. Fauchet, R. W. Collins, A. P. Alivisatos, I. Shimizu, T. Shimada, and J.-C. Vial, MRS Symposia Proceed-

ings No. 452 (Materials Research Society, Pittsburgh, 1997), p. 613.

[27] See, for example, J. P. Clerc, G. Giraud, J. M. Laugier, and J. M. Luck, Adv. Phys. **39**, 191 (1990).

[28] S. M. Sze, *Physics of Semiconductor Devices*, 2nd ed. (Wiley, New York, 1981).

[29] C. A. Neugubauer and M. B. Webb, J. Appl. Phys. **33**, 74 (1962).

[30] M. A. Lampert and P. Mark, *Current Injection in Solids* (Academic, New York, 1970).

[31] A. Rose, Phys. Rev. **97**, 1538 (1955).

[32] L. Tsybeskov, S. P. Duttagupta, K. D. Hirschman, and P. M. Fauchet, Appl. Phys. Lett. **68**, 2058 (1996).

[33] P. Gonon, A. Deneuville, F. Fontaine, and E. Greeraert, Appl. Phys. Lett. **78**, 6633 (1995).

[34] K. Natori, J. Appl. Phys. **78**, 4543 (1995).

[35] L. I. Glazman and R. I. Shekhter, J. Phys., Condens. Matter **1**, 5811 (1989).

[36] K. Yano, T. Ishii, T. Hashimoto, T. Kobayashi, F. Murai, and K. Seki, Appl. Phys. Lett. **67**, 828 (1995).

[37] K. Yano, T. Ishii, T. Hashimoto, T. Kobayashi, F. Murai, and K. Seki, IEEE Trans. Electron Devices **41**, 1628 (1994).

[38] S.-T. Ngiam, K. F. Jensen, and K. D. Kolenbrander, J. Appl. Phys. **76**, 8201 (1994).